JOURNAL OF AGRICULTURAL AND FOOD CHEMISTRY

Article

pubs.acs.org/JAFC

Kinetic and Thermodynamic Studies of Toluene, Ethylbenzene, and *m*-Xylene Adsorption from Aqueous Solutions onto KOH-Activated Multiwalled Carbon Nanotubes

Fei Yu,[†] Yanqing Wu,*[,†] Xiaoman Li,[†] and Jie Ma*[,§]

[†]School of Environmental Science and Engineering, Shanghai Jiao Tong University, Shanghai 200240, China

[§]State Key Laboratory of Pollution Control and Resource Reuse, School of Environmental Science and Engineering, Tongji University, Shanghai 200092, China

ABSTRACT: Multiwalled carbon nanotubes activated by KOH (CNTs-KOH) were synthesized and employed as adsorbents to study adsorption characteristics of toluene, ethylbenzene, and *m*-xylene (TEX) from aqueous solutions. Kinetics data were fitted by pseudo-second-order model, and intraparticle diffusion was not the only rate-controlling step. Adsorption isotherm data could fit well with Langmuir, Freundlich, and Dubinin−Radushkevich (D-R) models. The maximum adsorption capacities on CNTs-KOH are 87.12, 322.05, and 247.83 mg/g for toluene, ethylbenzene, and *m*-xylene, respectively. The adsorption capacities of TEX onto CNTs-KOH increased with contact time and decreased with temperature and are not significantly affected by humic acid. However, Cr^{6+} could decrease adsorption of TEX by 17.66, 4.51, and 12.69% as $(K_d^1 - K_d^2)/K_d^1$, respectively. The thermodynamics parameters indicated that adsorption was a feasible, exothermic, and spontaneous process in nature and a physisorption process. The present CNTs-KOH show a better EX adsorption performance than other adsorbents, suggesting that CNTs-KOH are promising EX adsorbents in wastewater treatment.

KEYWORDS: *adsorption, TEX, activated multiwalled carbon nanotube, kinetics, thermodynamics, chromium(VI)*

INTRODUCTION

Toluene, ethylbenzene, and *m*-xylene (TEX) are considered among the most prevalent groundwater pollutants. Human exposure to TEX can lead to health problems ranging from irritation of the eyes, mucous membranes, and skin, to weakened nervous systems, reduced bone marrow function, and cancers.[1] For many years, TEX has attracted widespread attention due to groundwater as the sole or major source of drinking water for many communities. Consequently, efficient treatment of TEX in groundwater is remarkably needed.

Carbon nanotubes (CNTs) were discovered by Iijima in 1991.[2] As adsorbents in the field of the environment, the adsorption of various inorganic and organic pollutants by CNTs was broadly studied, such as Pb,[3,4] Cd,[5,6] polyaromatics,[7,8] chlorophenols,[9] dyes,[10−12] diuron,[13] pharmaceutical antibiotics,[14] benzene, toluene, ethylbenzene, and xylene isomers (BTEX),[15−19] and 1-pyrenebutyric acid.[20] Earlier studies have reported the adsorption of TEX on CNTs.[15−19] Most of them focus on the adsorption properties of TEX onto multiwalled carbon nanotubes (MWCNTs) by various oxidized methods. The BET surface area greatly affects the adsorption properties, and the BET surface area of CNTs can be obviously enhanced by alkaline treatment.[21−23] However, few works have reported the adsorption of TEX onto CNTs by the activation treatment and simultaneously determined the equilibrium, kinetics, and thermodynamic parameters in aqueous solutions. Ji et al.[14] have reported that CNTs by KOH activation can improve the specific surface area (SSA) of CNTs and, thus, enhance adsorption of monoaromatic compounds and pharmaceutical antibiotics in aqueous solutions. An understanding of adsorption equilibrium, kinetics, and thermodynamics is critical in supplying the basic information required for the design and operation of adsorption. Therefore, this study elucidates the equilibrium, kinetics, and thermodynamics of the TEX adsorption onto KOH-activated CNTs.

In view of the foregoing, the objective of this study was to investigate TEX adsorption isotherms, kinetics, and thermodynamics on KOH-activated MWCNTs by using a batch technique from aqueous solutions. The adsorption rates were evaluated with the pseudo-first-order, pseudo-second-order, and intraparticle diffusion models. The Langmuir, Freundlich, and Dubinin−Radushkevich (D-R) isotherm models were used to fit the equilibrium data. The effects of humic acid and chromium(VI) on the adsorption behaviors were also investigated.

MATERIALS AND METHODS

Adsorbent Preparation. The present CNTs were prepared by the chemical vapor deposition (CVD)[24] method. Ethanol was used as carbon feedstock, ferrocene as catalyst, and thiophene as growth promoter. The synthesized temperature was 1000 °C. A non-destructive approach[25] was used to purify the pristine samples. The purified MWCNTs and KOH powder (KOH, 0.83 g; MWCNTs, 5 g) were mixed and ground for 10 min by a mortar. In a horizontal tube furnace under flowing argon, the activated reaction was performed in a stainless steel vessel at 1023 K for 1 h and then washed in concentrated HCl and deionized water and dried. The purified and activated MWCNTs are referred to as CNTs and CNTs-KOH,

Received: September 26, 2012
Revised: November 27, 2012
Accepted: November 27, 2012
Published: November 27, 2012

respectively, in the following text. The microstructure and morphology of adsorbents were analyzed by high-resolution transmission electron microscopy (HRTEM, JEOL 2100F, accelerating voltage of 200 kV). The BET surface area was determined from the adsorption−desorption isotherms of N_2 at 77 K using a BELSORP instrument (BEL, Japan, Inc.). The surface chemical properties were measured by X-ray photoelectron spectroscopic (XPS) analysis in a Kratos Axis Ultra DLD spectrometer, using monochromated Al Ka X-rays, at a base pressure of 1×10^{-9} Torr.

Batch Adsorption Experiments. All batch adsorption experiments were performed in 50 mL headspace bottles sealed with Teflon-lined screw caps. Twenty milligrams of CNTs-KOH was added to 50 mL of TEX solution of different initial concentrations at 283, 293, and 303 K. The initial concentrations were in the range of 9−60 mg/L for toluene, 11−83 mg/L for ethylbenzene, or 9−68 mg/L for *m*-xylene, and the initial pH was about 6. The mixture was shaken on a shaker (TS-2102C, Shanghai, China) at 180 rpm for 24 h. Blank experiments without adsorbents were conducted to ensure that the decrease in the concentration was actually due to the adsorption of CNTs-KOH, rather than the adsorption on the headspace bottle wall or via volatilization. All samples including blanks were run in duplicate, and the maximum deviation for the duplicates was usually <5%. At the end of the equilibrium period, the TEX concentration of the supernatant solutions was analyzed by gas chromatograph (GC 2010, Shinmadzu Corp., Japan) with flame ionization detection (GC-FID) using a DB-FFAP capillary column (30 m × 0.25 mm i.d., film thickness = 0.25 μm). The GC-FID was operated at an injection temperature of 523 K and a detector temperature of 523 K. The following temperature program was used: 323 K for 2 min and 283 K/min to 373 K.

The initial concentrations for adsorption kinetic studies were 40, 54, and 44 mg/L for toluene, ethylbenzene, and *m*-xylene, respectively. At predetermined time intervals, supernatants were analyzed by GC-FID. The predetermined times for dynamics were 10, 40, 60, 90, 180, 300, 420, and 600 min. The effect of humic acid and Cr^{6+} was also studied.

Experimental Analysis. The amount of adsorbed TEX on adsorbents (q_e, mg/g) was calculated as

$$q_e = (C_0 - C_e) \times \frac{V}{m} \tag{1}$$

where C_0 and C_e are the initial and equilibrium TEX concentrations (mg/L), respectively;V is the initial solution volume (L); and m is the adsorbent weight (g).

The most widely used kinetic models, that is, Lagergren first-order equation, pseudo-second-order equation, and intraparticle diffusion models, were used to investigate the kinetic adsorption behavior of TEX onto CNTs-KOH.[26] The best-fit model was selected on the basis of the determination coefficient (R^2) of the linear regression between the experimental data and the proposed models.

The Lagergren rate equation is one of the most widely used adsorption rate equations for the adsorption of solute from a liquid solution. The pseudo-first-order kinetic model of Lagergren may be represented by[27]

$$\log(q_e - q_t) = \log q_e - k_1 t \tag{2}$$

where q_e and q_t are the amounts of TEX adsorbed (mg/g) at equilibrium and time t (min), respectively, and k_1 is the rate constant of the pseudo-first-order kinetic model (min^{-1}). The values of q_e and k_1 can be determined from the intercept and the slope of linear plots of $\log(q_e - q_t)$ versus t.

A linear form of the pseudo-second-order kinetic model was expressed by[28]

$$\frac{t}{q_t} = \frac{1}{k_2 q_e^2} + \frac{1}{q_e} t \tag{3}$$

where q_e and q_t are the concentrations of TEX adsorbed on CNTs-KOH at equilibrium and at various times t and k_2 is the rate constant (g mg^{-1} min^{-1}) of the pseudo-second-order kinetic model for adsorption. Furthermore, the slope and intercept of the linear plot of t/q_t against t yielded the values of $1/q_e$ and $1/k_2 q_e^2$ for eq 3.

Because neither the pseudo-first-order nor the second-order model can identify the diffusion mechanism, the kinetic results were analyzed by the intraparticle diffusion model to elucidate the diffusion mechanism, which model is expressed as[29]

$$q_t = k_{id} t^{1/2} + C \tag{4}$$

where C(mg/g) is the intercept and k_{id} is the intraparticle diffusion rate constant (mg g^{-1} $min^{-1/2}$), which can be calculated from the slope of the linear plots of q_t versus $t^{1/2}$.

For adsorption isotherm study, Langmuir and Freundlich models were employed to fit the experimental data. The forms of Langmuir model and Freundlich model can be expressed respectively as

$$q_e = \frac{q_m K_L C_e}{1 + K_L C_e} \tag{5}$$

$$q_e = K_f C_e^{1/n} \tag{6}$$

where C_e and q_e are the concentrations of contaminants in water and adsorbent when the adsorption equilibrium was reached, respectively. q_m is the maximum adsorption capacity, and K_L is the Langmuir adsorption equilibrium constant (L/mg), which is related to the free energy of adsorption. K_f and n are Freundlich constants related to the adsorption capacity and adsorption intensity of the adsorbents ((mg/g)(L/mg)$^{1/n}$ and dimensionless).

To deepen the understanding of adsorption mechanism, the D-R isotherm model was chosen to apply on adsorption study. The D-R isotherm was applied to estimate the porosity apparent free energy and the characteristics of adsorption and can be used to describe adsorption on both homogeneous and heterogeneous surfaces. Its linear form is shown in eq 7

$$\ln q_e = \ln q_m - B\varepsilon^2 \tag{7}$$

where B is a constant related to the mean free energy of adsorption (mol^2 kJ^{-2}), q_m is the theoretical saturation capacity (mg/g), and ε is the Polanyi potential, which can be calculated from eq 8

$$\varepsilon = RT \ln(1 + 1/C_e) \tag{8}$$

where R (J mol^{-1} K^{-1}) is the gas constant and $T(K)$ is the absolute temperature. The slope of the plot of ln q_e versus ε^2 gives B (mol^2 kJ^{-2}), and the intercept yields the adsorption capacity,q_m. For the D-R isotherm equation, the mean free energy of adsorption (E_a), defined as the free energy change when 1 mol of ion is transferred from infinity in solution to the surface of the adsorbent, was calculated from the B value using the following relationship:

$$E_a = 1/(2B)^{1/2} \tag{9}$$

Thermodynamic parameters such as the change in Gibbs free energy ($\Delta G°$), enthalpy ($\Delta H°$), and entropy ($\Delta S°$) are calculated using the equations

$$\Delta G^\circ = -RT \ln K_0 \tag{10}$$

$$\ln K_0 = -\frac{\Delta H^\circ}{RT} + \frac{\Delta S^\circ}{R} \tag{11}$$

where K_0 is the thermodynamic equilibrium constant. As the TEX concentration in the solution decreases and approaches 0, values of K_0 are obtained by plotting a straight line of ln q_e/C_e versus q_e based on a least-squares analysis and extrapolation of q_e to 0. Subsequently, the intercept of the vertical axis gives the value of ln K_0. $\Delta H°$ is determined from the slope of the regression line after plotting ln K_0 against the reciprocal of absolute temperature, $1/T$. $\Delta G°$, $\Delta H°$, and $\Delta S°$ are determined from eqs 10 and 11, respectively.

RESULTS AND DISCUSSION

Physicochemical Characterization of MWCNTs. Figure 1 displays the surface morphology of CNTs and CNTs-KOH.

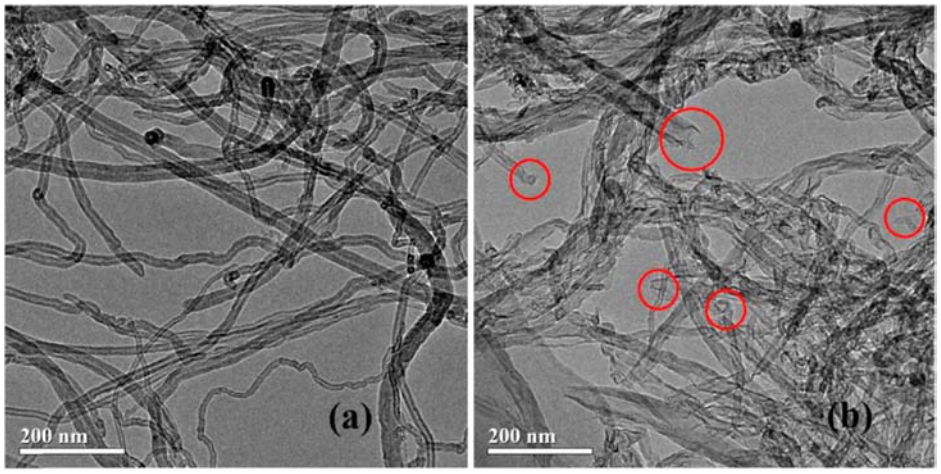

Figure 1. TEM of CNTs (a) and CNTs-KOH (b).

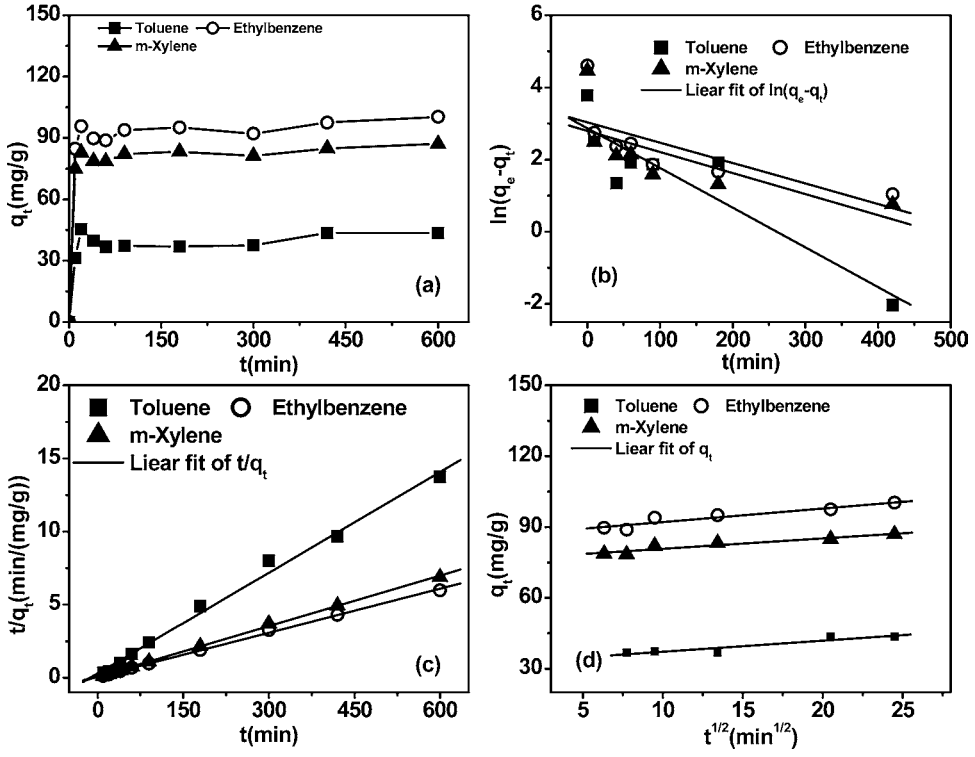

Figure 2. (a) Adsorption kinetics of TEX on CNTs-KOH (pH 6.0, at 20 °C); linear regressions of kinetics plots (b) pseudo-first-order model, (c) pseudo-second-order model, and (d) intraparticle diffusion model.

After KOH activation, the adsorbents still have a well-organized tube structure, cylindrical and hollow. Their outer diameters were approximately 20−30 nm. However, many small defects in the walls of CNTs-KOH have been evidently observed (red circles in Figure 2b). After activation by KOH, the BET surface area of CNTs increased from 123.5 to 534.6 m^2/g. After KOH-activated treatment, not only the tube tip was opened but also large quantities of new pore structures with small size were produced, which could give rise to a high BET surface area (Figure 2b). The samples are mainly made up of oxygen and carbon. After activation treatment, the weight content of surface oxygen of CNTs-KOH measured by XPS increased from 1.63 to 3.31 at. %. It is indicated that the functional groups are located on the surface of the CNTs-KOH.

Kinetic Analysis. It is important that kinetic study provided valuable information about the adsorption process and mechanism. As seen in Figure 2a, the adsorption progress is initially rapid and then becomes slow and stagnates with the increase in contact time, perhaps because a large number of vacant surface sites were available for adsorption during the initial stage and, then, the remaining vacant surface sites were difficult to occupy because of the repulsive forces between the TEX molecules on the CNTs-KOH and the bulk phase.[30]

To further investigate the adsorption processes of TEX on CNTs-KOH, adsorption kinetics analysis were conducted using the pseudo-first-order model, pseudo-second-order model, and intraparticle diffusion model. As shown in Figure 2b−d, three kinetic models are employed to fit the adsorption experimental data of TEX as well as other pollutants on solid adsorbents.[27,31]

Table 1. Kinetic Parameters of TEX Adsorbed on CNTs-KOH (pH 6.0 at 20 °C)

model	parameter	adsorbates		
		toluene	ethylbenzene	*m*-xylene
	C_0(mg/L)	39.52	54.02	43.64
	$q_{e,exptl}$(mg/g)	43.61	100.34	87.04
pseudo-first-order	k_1 (min^{-1})	0.011	0.0057	0.0058
	$q_{e,calcd}$(mg/g)	17.62	20.82	16.36
	R^2	0.794	0.454	0.436
pseudo-second-order	K_2(g mg^{-1} min^{-1})	0.00186	0.00161	0.00218
	$q_{e,calcd}$(mg/g)	43.48	99.50	86.51
	R^2	0.992	0.998	0.999
intraparticle diffusion	k_{id}(g mg^{-1} $min^{-0.5}$)	0.47	0.57	0.44
	C	32.45	86.43	76.46
	R^2	0.839	0.877	0.879

Table 1 presents the determination coefficients (R^2) of three models and the characteristic parameters.

The R^2 values of the pseudo-first-order were <0.9, but all of the experiment data showed better compliance with the pseudo-second-order kinetic model in terms of higher determination coefficient values (R^2 > 0.992). Moreover, the q values ($q_{e,calcd}$) calculated from the pseudo-second-order model were more consistent with the experimental q values ($q_{e,exptl}$) than those calculated by the pseudo-first-order model. Hence, the pseudo-second-order kinetic model was better fit to describe the adsorption behavior of TEX onto CNTs-KOH (Figure 2c), indicating that the chemical interactions were possibly involved in the adsorption processes and the adsorption capacity is proportional to the number of active sites on CNTs-KOH.[32,33] However, this study suggested that the thermodynamic analyses were more appropriate for determining whether the adsorption was a physisorption or a chemisorption process, as would be discussed in the following section.

Generally, the adsorption process on a porous adsorbent can be divided into three stages. The first stage is called external diffusion, in which the adsorbates move from the bulk solution to the external surface of the adsorbent; the second stage is the intraparticle diffusion, and the adsorbates diffuse further within the adsorbent to the adsorption sites; in the last stage, the adsorbates are adsorbed at the active sites on the adsorbent, which is a fast step and usually can be negligible.[34,35] As the pseudo-second-order model cannot identify the diffusion mechanism during the adsorption process, the intraparticle diffusion model was adopted to determine the adsorption kinetics of TEX onto CNTs-KOH.[36] It was essential for q_t versus $t^{1/2}$ plots to go through the origin if the intraparticle diffusion was the sole rate-limiting step.[35] As seen in Figure 2d, although the regression was linear after 40 min for ethylbenzene and *m*-xylene and after 60 min for toluene, the plot did not pass through the origin, indicating that intraparticle diffusion was related to the adsorption but not as a sole rate-controlling step.

Adsorption Isotherms. The equilibrium adsorption isotherms are some of the most important data to understand the mechanism of the adsorption systems and are useful to determine the amount of adsorbent needed to adsorb a required amount of adsorbate. Figures 3 and 4 show the adsorption isotherms and the simulation of TEX onto CNTs-KOH at three different temperatures. Adsorption equations were obtained from experimental data with Langmuir, Freundlich, and D-R models. The relative parameters calculated from the Langmuir and Freundlich models are listed in Table 2. It can be seen from Table 2 that the adsorption isotherms are fitted well by the three models except for the D-R model of toluene at 303 K. As shown in Figure 3, the adsorption capacities of TEX onto CNTs-KOH obviously decrease with

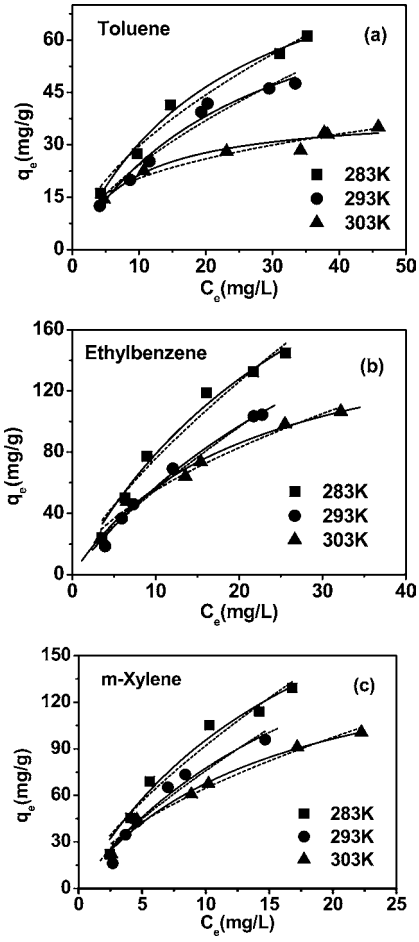

Figure 3. Adsorption isotherms of TEX on CNTs-KOH at pH 6: (a) toluene; (b) ethylbenzene; (c) *m*-xylene. The solid lines are Langmuir model; the dotted lines are Freundlich model.

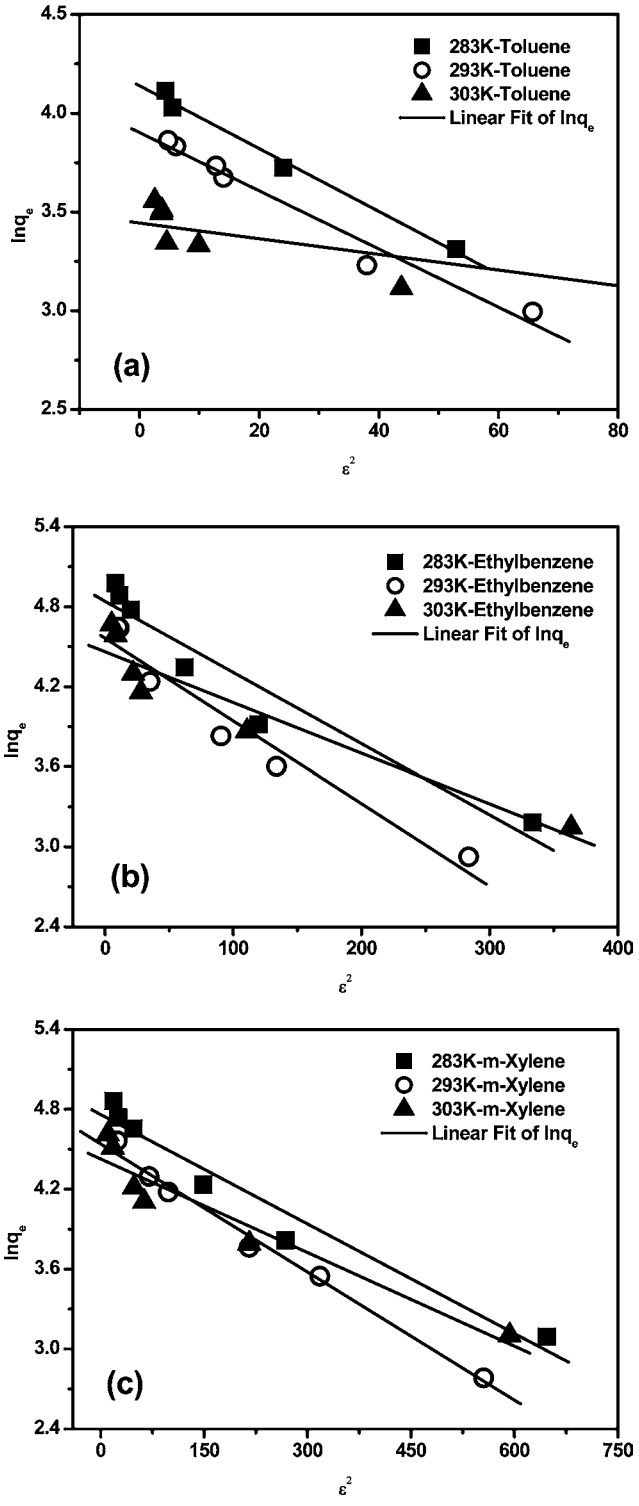

Figure 4. Linear fit of Dubinin–Radushkevich model for TEX on CNTs-KOH at different temperatures: (a) toluene; (b) ethylbenzene; (c) *m*-xylene.

the rise of temperature, which indicates that TEX adsorption onto CNTs-KOH is an exothermic reaction. According to the fitted results of Langmuir and D-R models, the adsorption capacity (q_m) also evidently decreases with temperature increase from 283 to 303 K. As the temperature increases from 283 to 303 K, the maximum adsorption capacities calculated by Langmuir model are 99.52, 87.12, and 39.63 mg/g for toluene, 339.37, 322.05, and 175.73 mg/g for ethylbenzene, and 278.28, 247.83, and 167.69 mg/g for *m*-xylene.

The adsorption capacities of the three adsorbates onto CNTs-KOH follow the order for different adsorbents, ethylbenzene > *m*-xylene > toluene, with different initial concentrations. The physiochemical properties of adsorbates play much important roles in adsorption characteristics. Favorable adsorption of that order of adsorbates may be attributed to the decrease in solubility (toluene, 515 mg/L > *m*-xylene, 175 mg/L > ethylbenzene, 152 mg/L), and the increase in molecular weight (MW, toluene, 92.15 < ethylbenzene, *m*-xylene, 106.18) and molar volume (Vs = MW/density, toluene, 106.69 < *m*-xylene, 122.25 < ethylbenzene, 122.44). The nature of monoaromatics is one factor influencing TEX adsorption performance.

The D-R isotherm model was chosen to deepen the understanding of the adsorption mechanism. The value of this parameter can give information about the adsorption mechanism. When 1 mol of matter is transferred, its value in the range of 1–8 kJ mol^{-1} shows physical adsorption;[37] the value of E_a is between 8 and 16 kJ mol^{-1}, which indicates the adsorption process follows by ion exchange, whereas its value in the range of 20–40 kJ mol^{-1} is indicative of chemisorption.[38] As seen in Table 2, the values of E_a are 5.61, 5.83, and 11.18 kJ mol^{-1} for toluene, 9.71, 8.98, and 11.47 kJ mol^{-1} for ethylbenzene, and 13.61, 12.5, and 14.74 kJ mol^{-1} for *m*-xylene at 283, 293, and 303 K, respectively. It seems that physical adsorption and ion exchange are dominating in the adsorption process of TEX onto CNTs-KOH. However, TEX usually exists in the form of molecules in the aqueous solutions, and thus ion exchange is not dominating in the TEX adsorption process onto CNTs-KOH. Moreover, the maximum capacity q_m obtained using the D-R isotherm model is lower than those experimental data. Therefore, chemical adsorption does not dominate in the adsorption process, and more information about the adsorption mechanism is needed.

Thermodynamic Studies. The thermodynamic parameters provide in-depth information on inherent energetic changes that are associated with adsorption; therefore, they should be properly evaluated. Thermodynamic parameters such as change in Gibbs free energy (ΔG°), enthalpy (ΔH°), and entropy (ΔS°) are calculated and given in Table 3. The negative ΔH° indicates the exothermic nature of the adsorption process for TEX on CNTs-KOH, which is supported by the decrease of TEX adsorption onto CNTs-KOH with a rise in temperature, as shown in Figure 3. The negative ΔG° suggests that the adsorption process is spontaneous with a high preference of TEX molecules for the CNTs-KOH and thermodynamically favorable. Furthermore, a more negative ΔG° implied a greater driving force of adsorption, resulting in a higher adsorption capacity (Figure 3 and Table 3). The negative ΔS° indicated the decrease in randomness at the solid/liquid interface during adsorption of TEX on CNTs-KOH.

The adsorption on solids is classified into physical adsorption and chemical adsorption, but the dividing line between the two is not sharp. However, physical adsorption is usually nonspecific, and the variation of energy for physical is usually substantially smaller than that of chemical reactions in that it is highly specific. Typically, ΔH° for physical adsorption ranges from −4 to −40 kJ mol^{-1}, compared to that of chemical adsorption ranging from −40 to −800 kJ mol^{-1}. Generally, ΔG° for physisorption is between −20 and 0 kJ/mol and for that for chemisorption is between −80 and −400 kJ/mol.[39] As

Table 2. Parameters of the Langmuir, Freundlich, and Dubinin−Radushkevich Models for Adsorption of TEX on CNTs-KOH at Different Temperatures (pH 6.0 at 20 °C)

	toluene			ethylbenzene			*m*-xylene		
parameter	10 °C	20 °C	30 °C	10 °C	20 °C	30 °C	10 °C	20 °C	30 °C
				Langmuir Model					
q_m(mg/g)	99.52	87.12	39.63	339.37	322.05	175.73	278.28	247.83	167.69
K_l(L/mg)	0.0439	0.0391	0.116	0.0302	0.0216	0.0476	0.0523	0.0455	0.0677
R^2	0.987	0.973	0.937	0.979	0.989	0.983	0.969	0.946	0.989
				Freundlich Model					
K_f(L/mg)	7.793	5.916	9.123	13.866	8.758	14.254	17.86	13.31	16.564
$1/n$	0.599	0.611	0.349	0.737	0.801	0.587	0.712	0.756	0.591
R^2	0.975	0.949	0.944	0.961	0.981	0.978	0.948	0.918	0.977
				Dubinin−Radushkevich Model					
q_m (mg/g)	62.78	49.52	31.31	126.62	95.84	86.6	116.91	93.66	83.71
B	0.0159	0.0147	0.004	0.0053	0.0062	0.0038	0.0027	0.0032	0.0023
E_a (kJ mol^{-1})	5.61	5.83	11.18	9.71	8.98	11.47	13.61	12.5	14.74
R^2	0.991	0.971	0.891	0.931	0.948	0.901	0.958	0.990	0.920

Table 3. Thermodynamic Parameters for TEX Adsorption onto CNTs-KOH (pH 6.0)

adsorbent	T (K)	ln K_0	$\Delta G°$ (kJ mol^{-1})	$\Delta H°$ (kJ mol^{-1})	$\Delta S°$ (J mol^{-1} K^{-1})
toluene	283	1.88	−4.42		−93.17
	293	1.25	−3.05	−30.79	−94.67
	303	1.02	−2.57		−93.14
ethylbenzene	283	2.65	−6.24		−61.13
	293	2.09	−5.09	−23.54	−62.96
	303	1.99	−5.03		−61.08
m-xylene	283	3.27	−7.69		−86.83
	293	2.6	−6.35	−32.27	−88.45
	303	2.37	−5.98		−86.77

shown in Table 3, $\Delta H°$ and $\Delta G°$ all implied that physisorption might dominate the adsorption of TEX onto CNTs-KOH.

Effect of Humic Acid on Adsorption. Currently, humic acid in drinking water is one of the accepted potential causes of Kashin−Bech disease in China.[40,41] Therefore, here the effect of humic acid on the adsorption of TEX is investigated. Humic acid (10 mg/L) was simultaneously added with TEX at an initial concentration range of 9−66 mg/L. The results are presented in Figure 5. In the presence of humic acid, the adsorption isotherms of toluene, ethylbenzene, and *m*-xylene have no significant differences compared to that of the absence of humic acid. Generally, humic acid could affect the adsorption of hydrophobic organic compounds (HOCs) onto CNTs by two major mechanisms. First, humic acid molecules may utilize adsorption sites on the surfaces of CNTs through direct site competition with HOC. Second, some humic acid molecules may be adsorbed into pores of CNTs, which are large enough to hold HOC molecules. Hence, pore blockage by humic acid may reduce the accessibility of HOC molecules to adsorption sites.[42] According to the results, neither pore blockage nor direct site competition for humic acid has an effect on TEX by CNTs-KOH. This is because that CNTs-KOH has the large BET surface area and porosity and TEX is small organic compound molecules. Humic acid has relatively lower steric restriction to prevent TEX molecules from approaching this adsorbent. Therefore, humic acid almost has no competition with TEX molecules on CNTs-KOH.

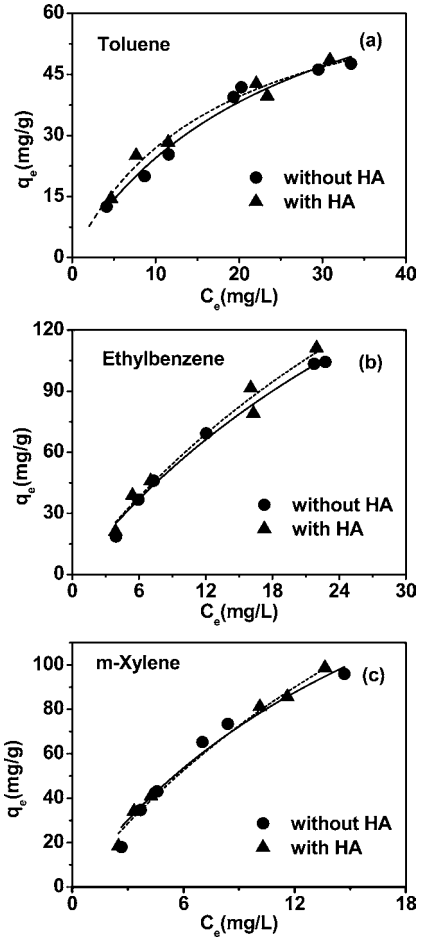

Figure 5. Effect of humic acid on TEX adsorption on CNTs-KOH: (a) toluene; (b) ethylbenzene; (c) *m*-xylene.

Effect of Cr^{6+} on TEX Adsorption. Heavy metals cause potential risk because of their impact on environmental quality and human health. As a representative, chromium(VI) is a highly toxic metal, which has been linked to cancer in humans and is also toxic to aquatic life at relatively low concentrations. Leaks, unsuitable storage, or improper disposal deposits of wastewaters containing chromium(VI) in the ground may lead to filtration and transport of the pollutant to groundwater sites.

To gain further insight into TEX adsorption onto CNTs-KOH, the effect of chromium(VI) on TEX adsorption was studied. The concentration of Cr^{6+} was 50 mg/L and TEX initial concentration was 30−50 mg/L. Figure 6 gives the results of

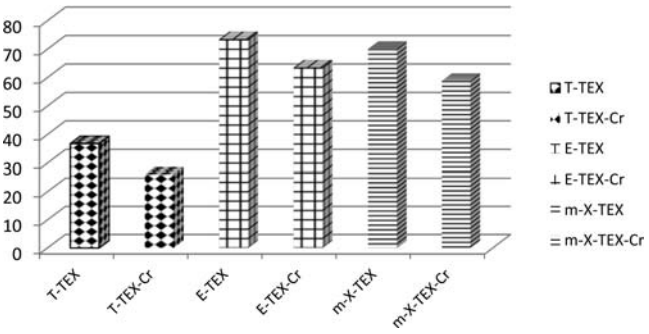

Figure 6. Effect of Cr^{6+} on adsorption capacity of TEX by CNTs-KOH.

the coadsorption of Cr^{6+} and TEX onto CNTs-KOH via adsorption capacity. It is obvious that the adsorption capacities of TEX are remarkably decreased in the presence of Cr^{6+} compared to that in the absence of Cr^{6+}. Therefore, Cr^{6+} significantly suppressed the adsorption of TEX onto CNTs-KOH. The impact of Cr^{6+} on TEX adsorption was expressed as $DI = (K_d^1 - K_d^2)/K_d^1$, where K_d^2 and K_d^1 correspond to the adsorption coefficients of TEX with and without Cr^{6+}, respectively (Table 4,; $K_d = q_e/C_e$). Cr^{6+} decreased the adsorption of toluene, ethylbenzene, and *m*-xylene onto CNTs-KOH by 17.66, 4.51, and 12.69%, respectively. This may be due to the formation of surface or inner-sphere complexes of Cr^{6+} through oxygen-containing functional groups and hydration, which may occupy some hydrophilic adsorption sites onto the surface of CNTs-KOH. The large metal cation hydration shells may intrude or shield the CNTs-KOH hydrophobic and hydrophilic sites and therefore indirectly compete with TEX for surface sites, leading to the inhibition of TEX adsorption around the metal-complexed moieties.

Table 4. Effect of Cr^{6+} on TEX Adsorption by CNTs-KOH

	K_d(L/kg)	inhibition (%)
T-TEX	1.41	
T-TEX-Cr	1.16	17.66
E-TEX	3.84	
E-TEX-Cr	3.67	4.51
m-X-TEX	6.32	
m-X-TEX-Cr	5.52	12.69

Comparison with Literature Results. The comparisons of TEX adsorption capacity by various adsorbents including single-walled carbon nanotubes (SWCNTs),[17] MWCNTs,[24,43] granular activated carbon (GAC),[44] activated carbon fiber (ACF),[45] angico sawdust,[46] peat,[46] and periodic mesoporous organosilica (PMO)[47] are summarized in Table 5. Under similar conditions, the adsorption capacity of toluene is not very high compared with other adsorbents in Table 5. However, the adsorption capacity of ethylbenzene and *m*-xylene is found to be relatively higher than most of the other adsorbents reported earlier, suggesting CNTs-KOH are suitable materials for the removal and preconcentration of EX from large volumes of aqueous solutions if CNTs could be produced in large scale at low price in the near future.

AUTHOR INFORMATION

Corresponding Author

*(Y.W.) E-mail: wuyanqing@sjtu.edu.cn. Phone: +86 21 34203731. Fax: +86 21 34203731. (J.M.) E-mail: jma@tongji.edu.cn. Phone: +86 21 65981831.

Funding

This research was supported by the Scholarship Award for Excellent Doctoral Student granted by the Ministry of Education and the Shanghai Jiao Tong University Innovation Fund for Postgraduates. This research was also supported by The National Natural Science Foundation of China (No. 41272261, 21207100), the State Key Laboratory of Pollution Control and Resource Reuse Foundation (No. PCRRY11009).

Notes

The authors declare no competing financial interest.

Table 5. Comparisons in TEX Adsorption of Various Adsorbents

	q_e(mg/g)				
adsorbent	toluene	ethylbenzene	*m*-xylene	conditions[a]	refs
CNTs-KOH	87.12	322.05	247.83	pH 6, T = 20	this study
SWCNT(NaOCl)[b,c]	103.2			pH 7, T = 25, C_0 = 200	17
CNTs-2.0%	44.9	61.12	62.82	pH 7, T = 20	24
CNTs-3.2%	99.47	115.63	112.19		
CNTs-4.7%	59.48	79.15	100.45		
CNTs-5.9%	31.28	40.18	48.73		
angico sawdust[d]	0.0185	4×10^{-7}	0.1111[e]		46
peat[d]	0.2564	0.0794	0.2174[e]		
PMO	5.147				47
ACF[c]	85	237		pH 7, T = 20, $C_0 \sim 100$	45
GAC[d,f]	194.1			pH 7, T = 30	44
GAC(HNO_3)[d]	122.3				
GAC[d]	221.13	250.65		pH 7, T = 25	
CNT(NaOCl)[d]	279.81	342.67			

[a] T = temperature (°C); C_0 = initial concentration (mg/L). [b] SWCNT = single-walled carbon nanotube. [c] Equilibrium adsorption capacity (mg/g). [d] Maximum adsorption capacity calculated from Langmuir model. [e] *m*-, *p*-xylenes. [f] GAC = granular activated carbon.

■ ACKNOWLEDGMENTS

We are thankful to the reviewers for their valuable comments to improve the manuscript.

■ REFERENCES

(1) Costa, A. S.; Romao, L. P. C.; Araujo, B. R.; Lucas, S. C. O.; Maciel, S. T. A.; Wisniewski, A.; Alexandre, M. R. Environmental strategies to remove volatile aromatic fractions (BTEX) from petroleum industry wastewater using biomass. *Bioresour. Technol.* **2012**, *105*, 31−39.

(2) Iijima, S. Helical microtubules of graphitic carbon. *Nature* **1991**, *354*, 56−58.

(3) Lin, D. H.; Tian, X. L.; Zhou, S.; Zhang, Z. Y.; He, X. A.; Yu, M. J. Metal impurities dominate the sorption of a commercially available carbon nanotube for Pb(II) from water. *Environ. Sci. Technol.* **2010**, *44*, 8144−8149.

(4) Vuković, G. D.; Marinković, A. D.; Škapin, S. D.; Ristić, M. Đ.; Aleksić, R.; Perić-Grujić, A. A.; Uskoković, P. S. Removal of lead from water by amino modified multi-walled carbon nanotubes. *Chem. Eng. J.* **2011**, *173*, 855−865.

(5) Cho, H.-H.; Wepasnick, K.; Smith, B. A.; Bangash, F. K.; Fairbrother, D. H.; Ball, W. P. Sorption of aqueous Zn[II] and Cd[II] by multiwall carbon nanotubes: the relative roles of oxygen-containing functional groups and graphenic carbon. *Langmuir* **2010**, *26*, 967−981.

(6) Vuković, G. D.; Marinković, A. D.; Čolić, M.; Ristić, M. Đ.; Aleksić, R.; Perić-Grujić, A. A.; Uskoković, P. S. Removal of cadmium from aqueous solutions by oxidized and ethylenediamine-functionalized multi-walled carbon nanotubes. *Chem. Eng. J.* **2010**, *157*, 238−248.

(7) Karanfil, T.; Zhang, S. J.; Shao, T.; Bekaroglu, S. S. K. The impacts of aggregation and surface chemistry of carbon nanotubes on the adsorption of synthetic organic compounds. *Environ. Sci. Technol.* **2009**, *43*, 5719−5725.

(8) Sheng, G. D.; Shao, D. D.; Ren, X. M.; Wang, X. Q.; Li, J. X.; Chen, Y. X.; Wang, X. K. Kinetics and thermodynamics of adsorption of ionizable aromatic compounds from aqueous solutions by as-prepared and oxidized multiwalled carbon nanotubes. *J. Hazard. Mater.* **2010**, *178*, 505−516.

(9) Shan, X. Q.; Chen, G. C.; Wang, Y. S.; Wen, B.; Pei, Z. G.; Xie, Y. N.; Liu, T.; Pignatello, J. J. Adsorption of 2,4,6-trichlorophenol by multi-walled carbon nanotubes as affected by Cu(II). *Water Res.* **2009**, *43*, 2409−2418.

(10) Yao, Y. J.; He, B.; Xu, F. F.; Chen, X. F. Equilibrium and kinetic studies of methyl orange adsorption on multiwalled carbon nanotubes. *Chem. Eng. J.* **2011**, *170*, 82−89.

(11) Ma, X. F.; Chang, P. R.; Zheng, P. W.; Liu, B. X.; Anderson, D. P.; Yu, J. G. Characterization of magnetic soluble starch-functionalized carbon nanotubes and its application for the adsorption of the dyes. *J. Hazard. Mater.* **2011**, *186*, 2144−2150.

(12) Yu, F.; Chen, J.; Chen, L.; Huai, J.; Gong, W.; Yuan, Z.; Wang, J.; Ma, J. Magnetic carbon nanotubes synthesis by Fenton's reagent method and their potential application for removal of azo dye from aqueous solution. *J. Colloid Interface Sci.* **2012**, *378*, 175−183.

(13) Deng, J.; Shao, Y.; Gao, N.; Deng, Y.; Tan, C.; Zhou, S.; Hu, X. Multiwalled carbon nanotubes as adsorbents for removal of herbicide diuron from aqueous solution. *Chem. Eng. J.* **2012**, *193*−*194*, 339−347.

(14) Ji, L. L.; Shao, Y.; Xu, Z. Y.; Zheng, S. R.; Zhu, D. Q. Adsorption of monoaromatic compounds and pharmaceutical antibiotics on carbon nanotubes activated by KOH etching. *Environ. Sci. Technol.* **2010**, *44*, 6429−6436.

(15) Lu, C. Y.; Su, F. S.; Hu, S. K. Adsorption of benzene, toluene, ethylbenzene and *p*-xylene by NaOCl-oxidized carbon nanotubes. *Colloid Surf. A*−*Physicochem. Eng. Asp.* **2010**, *353*, 83−91.

(16) Chin, C. J. M.; Shih, L. C.; Tsai, H. J.; Liu, T. K. Adsorption of o-xylene and p-xylene from water by SWCNTs. *Carbon* **2007**, *45*, 1254−1260.

(17) Zhu, D. Q.; Chen, W.; Duan, L. Adsorption of polar and nonpolar organic chemicals to carbon nanotubes. *Environ. Sci. Technol.* **2007**, *41*, 8295−8300.

(18) Lu, C.; Su, F.; Hu, S. Surface modification of carbon nanotubes for enhancing BTEX adsorption from aqueous solutions. *Appl. Surf. Sci.* **2008**, *254*, 7035−7041.

(19) Yu, F.; Ma, J.; Wu, Y. Q. Adsorption of toluene, ethylbenzene and *m*-xylene on multi-walled carbon nanotubes with different oxygen contents from aqueous solutions. *J. Hazard. Mater.* **2011**, *192* (3), 1370−1379.

(20) Rogers, R. E.; Bardsley, T. I.; Weinstein, S. J.; Landi, B. J. Solution-phase adsorption of 1-pyrenebutyric acid using single-wall carbon nanotubes. *Chem. Eng. J.* **2011**, *173*, 486−493.

(21) Chen, Y.; Liu, C.; Li, F.; Cheng, H.-M. Pore structures of multi-walled carbon nanotubes activated by air, CO_2 and KOH. *J. Porous Mater.* **2006**, *13*, 141−146.

(22) Raymundo-Pinero, E.; Azais, P.; Cacciaguerra, T.; Cazorla-Amoros, D.; Linares-Solano, A.; Beguin, F. KOH and NaOH activation mechanisms of multiwalled carbon nanotubes with different structural organisation. *Carbon* **2005**, *43*, 786−795.

(23) Lee, S. M.; Lee, S. C.; Jung, J. H.; Kim, H. J. Pore characterization of multi-walled carbon nanotubes modified by KOH. *Chem. Phys. Lett.* **2005**, *416*, 251−255.

(24) Yu, F.; Ma, J.; Wu, Y. Q. Adsorption of toluene, ethylbenzene and m-xylene on multi-walled carbon nanotubes with different oxygen contents from aqueous solutions. *J. Hazard. Mater.* **2011**, *192*, 1370−1379.

(25) Ma, J.; Wang, J. N. Purification of single-walled carbon nanotubes by a highly efficient and nondestructive approach. *Chem. Mater.* **2008**, *20*, 2895−2902.

(26) Chen, G. C.; Shan, X. Q.; Zhou, Y. Q.; Shen, X. E.; Huang, H. L.; Khan, S. U. Adsorption kinetics, isotherms and thermodynamics of atrazine on surface oxidized multiwalled carbon nanotubes. *J. Hazard. Mater.* **2009**, *169*, 912−918.

(27) Xiao, L.; Zhu, H. Y.; Jiang, R.; Zeng, G. M. Preparation, characterization, adsorption kinetics and thermodynamics of novel magnetic chitosan enwrapping nanosized γ-Fe_2O_3 and multi-walled carbon nanotubes with enhanced adsorption properties for methyl orange. *Bioresour. Technol.* **2010**, *101*, 5063−5069.

(28) Ngah, W. S. W.; Fatinathan, S. Adsorption of Cu(II) ions in aqueous solution using chitosan beads, chitosan-GLA beads and chitosan-alginate beads. *Chem. Eng. J.* **2008**, *143*, 62−72.

(29) Kavitha, D.; Namasivayam, C. Experimental and kinetic studies on methylene blue adsorption by coir pith carbon. *Bioresour. Technol.* **2007**, *98*, 14−21.

(30) Wu, C. H. Adsorption of reactive dye onto carbon nanotubes: equilibrium, kinetics and thermodynamics. *J. Hazard. Mater.* **2007**, *144*, 93−100.

(31) Yao, Y. J.; Xu, F. F.; Chen, M.; Xu, Z. X.; Zhu, Z. W. Adsorption behavior of methylene blue on carbon nanotubes. *Bioresour. Technol.* **2010**, *101*, 3040−3046.

(32) McKay, G.; Ho, Y. S. Pseudo-second order model for sorption processes. *Process Biochem.* **1999**, *34*, 451−465.

(33) Deng, S. B.; Yu, Q.; Zhang, R. Q.; Huang, J.; Yu, G. Sorption of perfluorooctane sulfonate and perfluorooctanoate on activated carbons and resin: kinetic and isotherm study. *Water Res.* **2009**, *43*, 1150−1158.

(34) Chingombe, P.; Saha, B.; Wakeman, R. J. Sorption of atrazine on conventional and surface modified activated carbons. *J. Colloid Interface Sci.* **2006**, *302*, 408−416.

(35) Yu, Q.; Zhang, R.; Deng, S.; Huang, J.; Yu, G. Sorption of perfluorooctane sulfonate and perfluorooctanoate on activated carbons and resin: kinetic and isotherm study. *Water Res.* **2009**, *43*, 1150−1158.

(36) Guibal, E.; McCarrick, P.; Tobin, J. M. Comparison of the sorption of anionic dyes on activated carbon and chitosan derivatives from dilute solutions. *Sep. Sci. Technol.* **2003**, *38*, 3049−3073.

(37) Onyango, M. S.; Kojima, Y.; Aoyi, O.; Bernardo, E. C.; Matsuda, H. Adsorption equilibrium modeling and solution chemistry depend-

ence of fluoride removal from water by trivalent-cation-exchanged zeolite F-9. *J. Colloid Interface Sci.* **2004**, *279*, 341−350.
(38) Tahir, S. S.; Rauf, N. Removal of a cationic dye from aqueous solutions by adsorption onto bentonite clay. *Chemosphere* **2006**, *63*, 1842−1848.
(39) Wu, C.-H. Adsorption of reactive dye onto carbon nanotubes: equilibrium, kinetics and thermodynamics. *J. Hazard. Mater.* **2007**, *144*, 93−100.
(40) Peng, A.; Wang, W. H.; Wang, C. X.; Wang, Z. J.; Rui, H. F.; Wang, W. Z.; Yang, Z. W. The role of humic substances in drinking water in Kashin-Beck disease in China. *Environ. Health Perspect.* **1999**, *107*, 293−296.
(41) Yao, Y. F.; Pei, F. X.; Kang, P. D. Selenium, iodine, and the relation with Kashin-Beck disease. *Nutrition* **2011**, *27*, 1095−1100.
(42) Wang, X. L.; Tao, S.; Xing, B. S. Sorption and competition of aromatic compounds and humic acid on multiwalled carbon nanotubes. *Environ. Sci. Technol.* **2009**, *43*, 6214−6219.
(43) Su, F.; Lu, C.; Hu, S. Adsorption of benzene, toluene, ethylbenzene and *p*-xylene by NaOCl-oxidized carbon nanotubes. *Colloids Surf., A* **2010**, *353*, 83−91.
(44) Wibowo, N.; Setyadhi, L.; Wibowo, D.; Setiawan, J.; Ismadji, S. Adsorption of benzene and toluene from aqueous solutions onto activated carbon and its acid and heat treated forms: influence of surface chemistry on adsorption. *J. Hazard. Mater.* **2007**, *146*, 237−242.
(45) Mangun, C. L.; Yue, Z.; Economy, J.; Maloney, S.; Kemme, P.; Cropek, D. Adsorption of organic contaminants from water using tailored ACFs. *Chem. Mater.* **2001**, *13*, 2356−2360.
(46) Costa, A. S.; Romão, L. P. C.; Araújo, B. R.; Lucas, S. C. O.; Maciel, S. T. A.; Wisniewski, A., Jr.; Alexandre, M. R. Environmental strategies to remove volatile aromatic fractions (BTEX) from petroleum industry wastewater using biomass. *Bioresour. Technol.* **2012**, *105*, 31−39.
(47) Moura, C. P.; Vidal, C. B.; Barros, A. L.; Costa, L. S.; Vasconcellos, L. C. G.; Dias, F. S.; Nascimento, R. F. Adsorption of BTX (benzene, toluene, *o*-xylene, and *p*-xylene) from aqueous solutions by modified periodic mesoporous organosilica. *J. Colloid Interface Sci.* **2011**, *363*, 626−634.